Computed Tomography Imaging Features in Acute Uncomplicated Stanford Type-B Aortic Dissection Predict Late Adverse Events

Anna M. Sailer, MD, PhD; Sander M.J. van Kuijk, PhD; Patricia J. Nelemans, MD, PhD; Anne S. Chin, MD; Aya Kino, MD; Mark Huininga, MD; Johanna Schmidt, PhD; Gabriel Mistelbauer, PhD; Kathrin Bäumler, PhD; Peter Chiu, MD; Michael P. Fischbein, MD, PhD; Michael D. Dake, MD; D. Craig Miller, MD; Geert Willem H. Schurink, MD, PhD; Dominik Fleischmann, MD

Background—Medical treatment of initially uncomplicated acute Stanford type-B aortic dissection is associated with a high rate of late adverse events. Identification of individuals who potentially benefit from preventive endografting is highly desirable.

Methods and Results—The association of computed tomography imaging features with late adverse events was retrospectively assessed in 83 patients with acute uncomplicated Stanford type-B aortic dissection, followed over a median of 850 (interquartile range 247–1824) days. Adverse events were defined as fatal or nonfatal aortic rupture, rapid aortic growth (>10 mm/y), aneurysm formation (≥6 cm), organ or limb ischemia, or new uncontrollable hypertension or pain. Five significant predictors were identified using multivariable Cox regression analysis: connective tissue disease (hazard ratio [HR] 2.94, 95% confidence interval [CI]: 1.29–6.72; *P*=0.01), circumferential extent of false lumen in angular degrees (HR 1.03 per degree, 95% CI: 1.01–1.04, *P*=0.003), maximum aortic diameter (HR 1.10 per mm, 95% CI: 1.02–1.18, *P*=0.015), false lumen outflow (HR 0.999 per mL/min, 95% CI: 0.998–1.000; *P*=0.055), and number of intercostal arteries (HR 0.89 per n, 95% CI: 0.80–0.98; *P*=0.024). A prediction model was constructed to calculate patient specific risk at 1, 2, and 5 years and to stratify patients into high-, intermediate-, and low-risk groups. The model was internally validated by bootstrapping and showed good discriminatory ability with an optimism-corrected C statistic of 70.1%.

Conclusions—Computed tomography imaging-based morphological features combined into a prediction model may be able to identify patients at high risk for late adverse events after an initially uncomplicated type-B aortic dissection. **(*Circ Cardiovasc Imaging*. 2017;10:e005709. DOI: 10.1161/CIRCIMAGING.116.005709.)**

Key Words: aneurysm ■ aorta ■ aortic rupture ■ computed tomography angiography ■ hypertension ■ regression analysis

Patients with initially uncomplicated Stanford type-B aortic dissection (AD) who survive the acute event without the need for open or endovascular intervention before hospital discharge have a relatively benign short-term course. The reported survival under optimal medical therapy (OMT) is 90% to 95% within the first few months.[1–5] OMT fails to prevent aortic wall degeneration and disease progression, however, necessitating life-long surveillance. Between 20% and 65% of patients with initially uncomplicated type-B AD develop late complications within 5 years.[6–10]

See Editorial by LaBounty and Eagle
See Clinical Perspective

Thoracic endovascular aortic repair (TEVAR) has been postulated to prevent late complications based on the observation that endografting leads to false lumen thrombosis and favorable aortic remodeling.[11,12] Both effects have been confirmed in prospective trials, but did not translate into a survival benefit in the first 2 years after TEVAR.[13,14] Preemptive endografting of all patients with uncomplicated type-B AD would thus expose many low-risk patients to the low but potentially devastating risk of procedural complications—such as stroke or paraplegia[15–17]—without conveying a tangible benefit.

Several investigators have sought to identify clinical or imaging-based morphological predictors for progressive false lumen aneurysmal dilatation to identify individuals at high risk

Received September 21, 2016; accepted February 16, 2017.

From the Department of Radiology (A.M.S., A.S.C., A.K., K.B., D.F.), Department of Cardiothoracic Surgery (P.C., M.P.F., M.D.D., D.C.M.), and the Stanford Cardiovascular Institute (M.D.D., D.F.), Stanford University School of Medicine, CA; Department of Radiology (A.M.S.), Department of Clinical Epidemiology and Medical Technology Assessment (S.M.J.v.K.), Department of Epidemiology (P.J.N.), and Department of Vascular Surgery (M.H., G.W.H.S.), Maastricht University Medical Center, The Netherlands; Institute of Simulation and Graphics, Otto von Guericke University Magdeburg, Germany (G.M.); and the Institute for Computer Graphics, Vienna University of Technology, Austria (J.S., G.M.).

Correspondence to Dominik Fleischmann, MD, Department of Radiology, Stanford University School of Medicine, 300 Pasteur Dr, S-072, Stanford, CA 94305. E-mail d.fleischmann@stanford.edu

for adverse events (AEs).[18–32] To the best of our knowledge, no attempt has been made to analyze the presumed and known risk factors simultaneously and build a single prediction model for individual risk stratification. This is highly desirable because high-risk patients are more likely to benefit from early TEVAR, whereas non–high-risk patients likely fare better with OMT.

The purpose of this study was therefore to determine the association of clinical and imaging-based morphological and functional features obtained during the index hospitalization with late AEs in patients with initially uncomplicated type-B AD, and to derive a model for prediction of individual risk for late AEs.

Methods

This study was approved by the institutional review boards of the participating institutions. The requirement of obtaining informed consent was waived given the retrospective nature of this work.

Patient Selection

Patients were retrospectively identified from the surgical and imaging databases of 2 aortic centers in the United States and Europe. Two-hundred seven patients who had presented to 1 of the 2 participating institutions with acute type-B AD or intramural hematoma between January 2002 and December 2012, and who survived the initial hospitalization without complications requiring surgical or endovascular intervention were initially reviewed. All patients were treated with OMT and underwent at least 1 computed tomography (CT) scan during or immediately before the index hospitalization.

Clinical data from the index hospitalization and all follow-up encounters were reviewed from the electronic medical records. Patients were classified as having an AE if 1 or more of the following events occurred after hospital discharge: fatal or nonfatal aortic rupture, organ or limb ischemia, aortic aneurysm formation (defined as the maximum thoracic aortic diameter ≥6 cm), rapid aortic growth (defined as diameter increase of ≥10 mm within 1 year), and new refractory hypertension or pain, uncontrollable by medical management.

Imaging Data

All imaging data were retrieved from the local picture archiving and communication systems of the participating sites and transferred to an independent 3D server (iNtuition, TeraRecon, Inc, Foster City, CA). CT angiograms obtained at the time of the index hospitalization were reviewed by 2 experienced cardiovascular radiologists in consensus. Studies were read in the order of event date, with readers unaware of patient outcomes. If more than 1 CT scan was available in the acute phase (eg, from an outside institution immediately before transfer, or an admission CT and a predischarge CT), the scan with the highest diagnostic quality was used for evaluation. Routine follow-up CT scans were obtained at 3, 6, and 12 months, and annually thereafter, but intervals could vary between patients. Follow-up CT scans were reviewed by 1 or 2 cardiovascular radiologists in all patients. Standardized aortic diameter measurements were obtained on all index and follow-up scans using iNtuition software. The maximum aortic diameter was obtained in a cross-sectional plane perpendicular to the aortic centerline (Figure 1).

Morphological Characteristics on CT Imaging

We sought to explore a wide range of imaging features observed in the acute phase as candidate morphological predictors for late AEs, including all features which have been previously described as potential causes of complications in patients with AD.[18–32] These features refer to the aortic diameter, the size, location and number of primary entry tears, and the size, extent, and relative location of the true and false lumen within the dissected aorta. Features related to the false lumen, such as number of channels and false lumen thrombosis, were also considered. The imaging features included in our analysis after eliminating redundant descriptions are listed in Table 1. Each feature was defined according to its most detailed original description.

We introduced a new measurement for the relative sizes of the true versus false lumen: rather than diameters or shapes (circular versus elliptical)[30,31] which are affected by the mobility of the dissection membrane over the cardiac cycle, we measured the circumferential extent of the false lumen in angular degrees along the outer aortic wall (Figure 2). Measurements were obtained on the same orthogonal cross-section where the aortic diameter was the maximum. This parameter, referred to as the false lumen circumferential extent, is unaffected by the variable position of the dissection membrane, and attempts to capture the physiology of the dissection by quantifying the proportion of weakened outer aortic wall exposed to false lumen pressure versus the proportion of preserved outer aortic wall circumference exposed to true lumen pressure.

Because progressive false lumen dilatation is a preeminent long-term complication in patients with chronic AD,[33] we also explored new features thought to be related to chronic false lumen pressurization. Early experimental and invasive angiographic observations in patients with acute malperfusion syndromes suggest that both the diastolic and mean pressures in the false lumen are strongly related to the total resistance of available outflow channels.[34–36] Extrapolating to chronic dissection, we would expect a more rapid progression of aortic dilatation in patients with limited outflow from the false lumen, and a slower progression in patients with adequate false lumen drainage. Conceptually, the false lumen can be drained by supplying blood to large vessels (such as visceral and renal arteries) or small vessels (intercostal and lumbar branches), and by large or small communications between the true and false lumen.

In an attempt to estimate the relative blood flow emanating from the false lumen, we identified the left subclavian artery, the visceral arteries (celiac, superior, and inferior mesenteric), the renal, and the common iliac arteries in all patients. Each branch artery was classified as arising from the true lumen, the false lumen, or both, based on the relative position to the respective aortic channels and the observed pattern of enhancement. The total false lumen outflow was estimated as the sum of presumed blood flow to each branch supplied by the false lumen. Based on reference data for resting blood flow in humans,[37] we assumed left subclavian artery flow as 275 mL/min, the celiac and superior mesenteric artery flow as 550 mL/min each, left and right renal artery flow as 500 mL/min each, the inferior mesenteric artery as 190 mL/min, and the iliac arteries as 400 mL/min each. If a vessel originated from both channels, the flow was equally split between both, the true and false lumen, respectively. Completely occluded branches were not scored.

Finally, we recorded all identifiable intercostal arteries arising off the thoracic aorta, and lumbar arteries arising off the abdominal aorta. An attempt was made to identify the true lumen, the false lumen, or both as the origin of each of these small branches, but this was not always possible. No specific attempt was made to measure communications between the true and false lumen, because this was deemed unreliable in the presence of motion artifacts. We also expected that transmembrane communications would be captured—at least in part—by recognizing the false lumen branch supply, because each branch off the false lumen is necessarily associated with a corresponding fenestration in the dissection membrane.

Development of a Risk-Prediction Model

Baseline characteristics of the study group were presented as means and SDs, or absolute number and percentages, where appropriate. Multivariable Cox regression analysis was used to evaluate the associations between candidate clinical and morphological predictors and the occurrence of AEs taking into account the correlations among variables. Restricted cubic splines were applied to estimate nonlinear relationships of the continuous predictors with AEs. After initial selection of candidate predictors based on their frequency distributions and after elimination of redundant candidates, the final selection of predictors was performed by backward stepwise elimination using a liberal P value for the Wald test of $P<0.157$, based on Akaike's Information Criterion to prevent too early deletion of potential predictors (or underfitting of the model).[38] The correlation between the

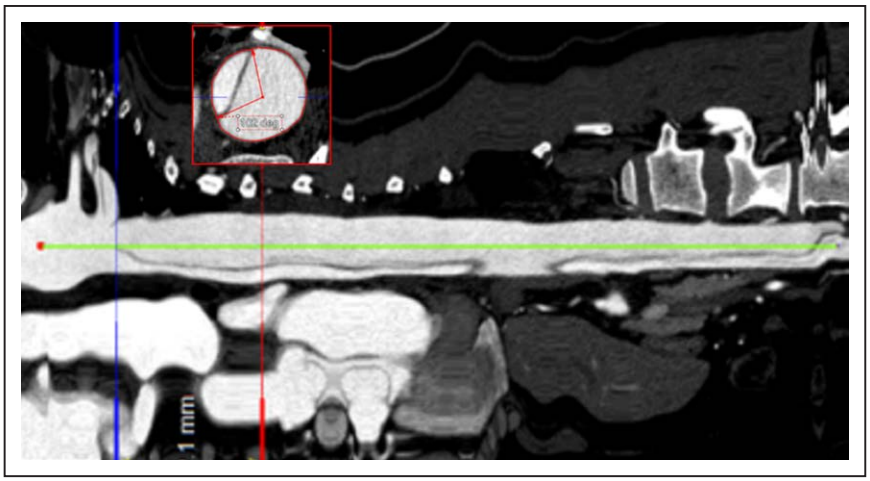

Figure 1. Three-dimensional assessment of maximum aortic diameter and circumferential extent false lumen. After generation of an aortic centerline (green line) from the proximal aortic arch to the aortic bifurcation the aorta is straightened along its centerline in a patient with uncomplicated type-B aortic dissection. Blue line indicates the distal ostium of the left subclavian artery. The red line indicates the location of the maximum diameter of the aorta. The aortic cross-section (inset) is oriented orthogonal to the aortic centerline. Inset, A false lumen circumferential extent of 258° (360°–102°) at this location.

scaled Schoenfeld residuals and time were computed to test the proportional hazards assumption.[39]

Model Performance and Validation

The concordance statistic (C statistic) was used to evaluate the ability of the model to discriminate between patients who will develop AEs and those who will not develop an AE. The C statistic ranges from 0.5 (indicating no discriminative ability) to 1.0 (indicating perfect discriminative ability). The calibration of the model was assessed by visually inspecting a calibration plot that was obtained by resampling in which predicted probabilities are plotted against actual probabilities. As an internal validation step, bootstrapping was performed to correct for overfitting by shrinking the coefficients of the model, and to correct for optimism in the performance parameters. This method is considered more efficient than split-sample and cross-validation methods.[40] A total of 1000 bootstrap samples were drawn from the original sample to mimic drawing samples from the underlying population. Estimates of optimism in the performance measures of the prediction model were subsequently subtracted from the original estimates. In addition, regression coefficients were multiplied by a shrinkage factor. These adjustments result in less extreme predictions for future patients and counteract too extreme predictions caused by overfitting of the model.

Estimation of Individual Absolute and Relative Risk

The linear predictor—or risk score—was calculated for each individual as the sum of the regression coefficients multiplied by the observed values on the corresponding predictor variable for that individual (ie, $\beta_1 \times X_1 + \beta_2 \times X_2 + \ldots + \beta_k \times X_k$). In the typical situation of an event being an adverse outcome, a high score indicates a worse prognosis. If the baseline survival function of a population is known, the individual risk score can be used to estimate the absolute probability of an AE for a given individual and point in time. Alternatively, the risk score can be used to categorize patients into different relative risk groups according to their rank into high-, intermediate-, and low-risk groups of equal size. A Kaplan–Meier curve was constructed to illustrate the differences in the observed risk of AEs between the 3 risk groups.

Results

Of 207 patients with acute uncomplicated type-B AD or intramural hematoma treated at the 2 participating centers, 71 were managed at outside facilities after hospital discharge. The remaining 136 of 207 patients were followed at one of the participating centers, 80 patients at center A, and 56 patients at center B. Patients with intramural hematoma (n=44), iatrogenic dissection (n=3), and patients with isolated abdominal AD (n=6) were excluded from the analysis. The final study population consisted of 83 patients (47 patients from center A and 36 patients from center B), 58 men (70%), and 25 women (30%), with a mean age of 54 years (Table 1). Fourteen patients had connective tissue diseases, including the Marfan syndrome (n=12), Ehlers–Danlos syndrome (n=1), and Loeys-Dietz Syndrome (n=1). Patients were followed for a median of 850 days (interquartile range 247–1824). All 83 patients had at least 1 follow-up scan after discharge from the index hospitalization. In 76 of 83 patients (92%), 2 or more follow-up CT scans were available. In 45 patients (54%), 5 or more follow-up CT scans were available. AEs were observed in 33 of 83 (40%) patients: 17 patients developed aneurysms (maximum aortic diameter ≥6 cm), an additional 8 patients demonstrated rapid aortic growth (≥10 mm/y), 4 patients developed renal ischemia, 2 patients developed limb ischemia, 1 patient developed bowel ischemia, and 1 patient presented with aortic rupture. Twenty-one of 83 patients exceeded at least 5 years of follow-up, 29 of 83 patients (35%) were censored without an event (all lost to follow-up). The actual sample sizes for each year (individuals at risk) are provided in the Kaplan–Meier Analysis.

Risk-Prediction Model

The distribution of clinical and candidate morphological predictors identified at imaging in the acute phase is presented in Table 1.

The restricted cubic spline regression yielded no nonlinear associations, and none of the predictors violated the proportional hazards assumption. The multivariable selection of candidate predictor variables yielded 5 significant predictors of AEs: connective tissue disease, circumferential extent of the false lumen in angular degrees, maximum aortic diameter in millimeters, false lumen outflow in milliliters per minute, and total number of intercostal arteries. The hazard ratios with confidence intervals and the uncorrected and shrunk regression coefficients are presented in Table 2 and Figure 3. All selected predictor variables met the proportional hazards assumption.

Model Performance and Internal Validation

The C statistic of the model was 73.8% (95% confidence interval: 62.2%–85.2%). Figure 4 shows the calibration plot of the model at 2 years follow-up. The optimism-corrected calibration line lies close to the line of perfect calibration. It shows a slight underestimation of risk for patients at relatively low

Table 1. Distribution of Patient Characteristics and Morphological Characteristics on CT Imaging at Index Hospitalization of Patients With Uncomplicated Type-B ADs

Patient characteristics	Type-B AD (n=83)
Age, y	54.0±15.5
Male sex	58 (70%)
Connective tissue disease	14 (17%)
Hypertension*	71 (86%)
Hyperlipidemia*	32 (39%)
Diabetes mellitus*	6 (7%)
Smoking (active and former)*	44 (53%)
CT characteristics	Type-B AD (n=83)
Lumina	
False lumen thrombosis	Complete: 0 (0%), partial: 39 (47%), patent: 44 (53%)
Location of the true lumen in the distal arch*	Inner curvature: 79 (95%) outer curvature: 4 (5%)
Circumferential extent of false lumen, °	249.3±39.9
Thin moving intimal flap*	77 (93%)
Multichannel dissection*	3 (4%)
Dissection	
Length of the dissection, cm*	37.2±11.1
Extent of the dissection*	Thoracic: 11 (13%), thoraco-abdominal: 72 (87%)
Aortic diameters	
Maximum diameter of the dissection, cm	37.0±5.4
Diameter of false lumen at maximum aortic diameter, cm	20.7±6.4
Fusiform index>0.64*	5 (6%)
Intimal tear	
Distance primary tear from left subclavian artery, cm*	7.6±4.6
Anatomic location primary intimal tear	Distal arch concavity: 22 (27%), distal arch convexity 24 (29%), distal arch concavity-convexity 2 (2%), mid-descending: 23 (28%), distal descending: 12 (15%)
Maximum diameter of primary intimal tear, mm	9.1±5.9
Number of tears	1.4±0.6
Outflow over the length of the dissection	
Left subclavian artery*	TL: 2 (2%), FL: 0 (0%), both: 6 (7%)
Celiac trunk*	TL: 50 (60%), FL: 11 (13%), both: 12 (15%)
Superior mesenteric artery*	TL: 63 (76%), FL: 3 (4%), both: 5 (6%)
Left renal artery*	TL: 35 (42%), FL: 27 (33%), both: 5 (6%)
Right renal artery*	TL: 46 (55%), FL: 12 (15%), both: 8 (10%)
Inferior mesenteric artery*	TL: 36 (43%), FL: 18 (22%), both: 2 (2%)
Left iliac artery*	TL: 19 (23%), FL: 4 (5%), both: 29 (35%)
Right iliac artery*	TL: 20 (24%), FL: 2 (2%), both: 30 (36%)
Number of intercostal arteries from true and false lumen	11.7±3.7
Number of lumbar arteries from true and false lumen	6.2±3.8
Large vessel outflow volume from true lumen, mL*	1766±902
Large vessel outflow volume from false lumen, mL	650±452

AD indicates aortic dissection; CT, computed tomography; FL, false lumen; and TL, true lumen.

*Characteristic not selected as candidate for stepwise backward selection.

risk of AEs, whereas the model is well calibrated for patients at higher risk for an AE.

The bootstrap internal validation yielded a shrinkage factor of 0.78. The regression coefficients were multiplied by the shrinkage factor to obtain the model penalized for overfitting (Table 2). The optimism-corrected C statistic, which is an estimate of the C statistic of the model when applied to future patients, was 70.1%.

Estimation of Individual Absolute and Relative Risk

The individual absolute probability of an AE within 1, 2, or 5 years can be calculated based on a patient's linear predictor if the baseline survival function of a population is known. The linear predictor is calculated using the centered predictor values (ie, the mean values are subtracted from the observed values): 0.841×(connective tissue disease−0.169)+0.021×(false lumen circumferential extent−249)+0.071×(maximum aortic diameter−37)−0.001×(false lumen outflow−650)×0.094×(number of intercostals−11.7). In our study population, the estimated baseline survival was 0.898, 0.815, and 0.631 at 1, 2, and 5 years, respectively. The individual 1-, 2-, and 5-year probability of survival without an AE is calculated as (baseline survival)$^{\exp(\text{linear predictor})}$, and the corresponding 1-, 2-, and 5-year risk of an AE is (1−baseline survival)$^{\exp(\text{linear predictor})}$.

For example, the linear predictor for a patient without connective tissue disease, 260° of false lumen circumferential extent, 40 mm maximum aortic diameter, 550 mL/min of false lumen outflow, and 7 patent intercostal arteries in the area of the dissection is as follows: 0.841×(0−0.169)+0.021×(260−249)+0.071×(40−37)−0.001×(550−650)−0.094×(7−11.7)=0.844. The 1-year probability of event-free survival in this patient is estimated at $(0.898)^{\exp(0.844)}$=0.78 and the risk

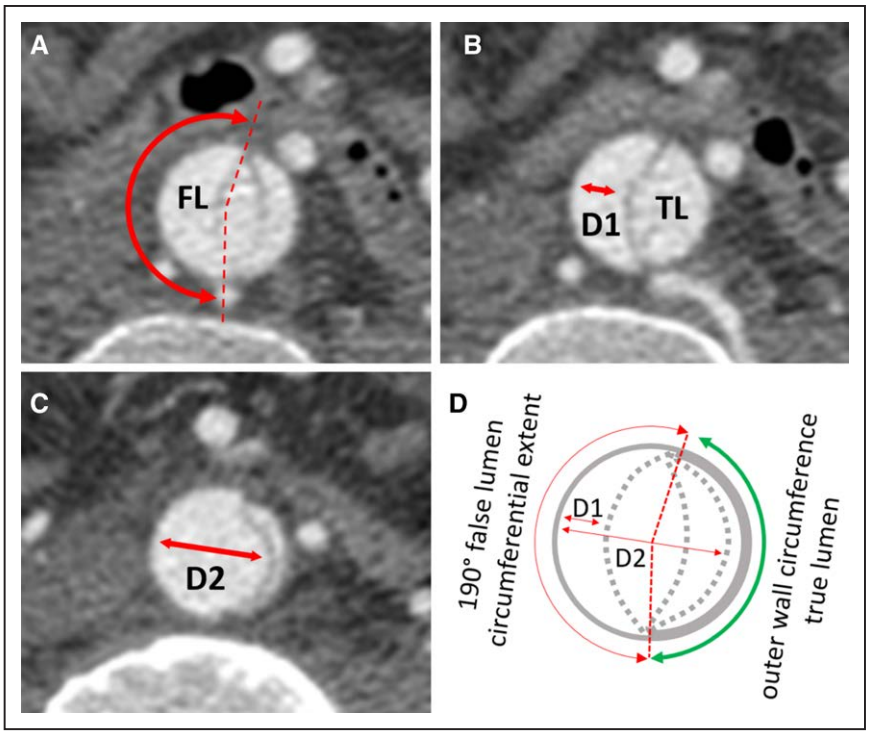

Figure 2. Measurement of the false lumen (FL) circumferential extent of detachment in aortic dissection. **A**–**C**, A mobile dissection membrane separating the FL from the true lumen (TL) in different positions on 3 contiguous images of the abdominal aorta in a patient with aortic dissection. Note the double contours of the dissection membrane in **A**, the smaller diameter (*D*1) in **B**, and the largest diameter (*D*2) of the FL in **C**. The schematic in **D** shows that the 190° circumferential extent of the FL in angular degrees remains constant over the cardiac cycle, despite the variable location of the dissection flap (dotted lines) and thus diameter measurements.

of an event is $1-((0.898)^{\exp(0.844)})=1-0.78=0.22$. The 2- and 5-year risks of an AE are 0.38 and 0.66, respectively.

If the baseline survival function is not known, it is possible to rank patients according to a relative risk score and to subsequently classify them into relative risk groups. This is illustrated in Figure 5 where the Kaplan–Meier curves show event-free survival stratified by tertiles of the linear predictor. These predictor values were not centered, to keep calculation straightforward. Scores up to 6.05 are classified as low risk, scores between 6.06 and 7.0 as intermediate risk, and scores greater than 7.0 as high risk for an adverse event, respectively. Risk score=0.841×(connective tissue disease)+0.021×(false lumen circumferential extent)+0.071×(maximum aortic diameter)–0.001×(false lumen outflow)–0.094×(number of intercostals). Thus, the example patient with a score of 7.092 (0.841×0+0.021×260+0.071×40–0.001×550–0.094×7=7.092) would be classified as high risk. The median event-free survival time was 3150 days (or 8.6 years), 2457 days (or 6.7 years), and 702 days (or 1.9 years) for the low-, intermediate-, and high-risk groups, respectively. The average risk for an AE before 2 years was 7.4%, 20.6%, and 54.4%, for the low-, intermediate-, and high-risk groups, respectively, in this population. Because the time-to-event analysis in our cohort is based on the same events used to create the model, the absolute risks may differ in populations with different baseline survival functions.

Discussion

This study was motivated by the renewed interest in the problem of how to best treat patients with initially uncomplicated Stanford type-B ADs. Although traditional OMT with anti-impulse therapy has acceptable short-term prognosis, long-term effectiveness is limited by chronic false lumen

Table 2. Regression Coefficients and HR With 95% CI Corresponding With Selected Variables for Prediction Model for Adverse Events in Uncomplicated Type-B AD

Variable	Regression Coefficient	HR (95% CI)	Shrunk Regression Coefficient*	*P* Value†
Connective tissue disease (yes)	1.078	2.94 (1.29–6.72)	0.841	0.01
False lumen circumferential extent, °	0.026	1.03 (1.01–1.04)	0.021	0.003
Maximum aortic diameter, mm	0.091	1.10 (1.01–1.04)	0.071	0.015
False lumen outflow, mL/min	–0.001	0.999 (0.998–1.000)	–0.001	0.055
Number of intercostals, n	–0.120	0.89 (0.80–0.98)	–0.094	0.024

Selection of variables was based on backward stepwise elimination. The individual probability of an adverse event within 1, 2, or 5 y can be calculated as: $(1-\text{baseline survival}^{\exp(\text{linear predictor})})\times 100\%$, in which the baseline survival for 1, 2, and 5 y are 0.898, 0.815, and 0.631, respectively, and the linear predictor=0.841×(connective tissue disease–0.169)+0.021×(false lumen circumferential extent–249)+0.071×(maximum aortic diameter–37)–0.001×(false lumen outflow–650)–0.094×(number of intercostals–11.7). AD indicates aortic dissection; CI, confidence interval; and HR, hazard ratio.

*Adjustment for overfitting by shrinkage (shrinkage factor=0.78).

†A liberal *P* value for the Wald test of $P<0.157$ based on Akaike's Information Criterion is used.

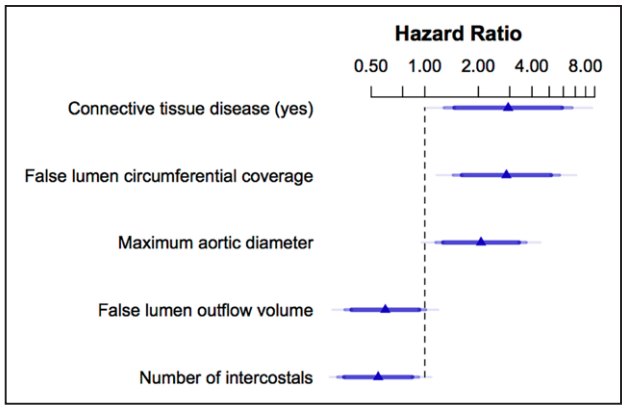

Figure 3. Hazard ratios of the 5 significant predictors selected by backward stepwise elimination. Shades of blue indicating the 90%, 95%, and 99% confidence intervals.

aneurysm degeneration over time and a high rate of late complications.[1–10] Although endovascular repair has a favorable effect on false lumen thrombosis and aortic remodeling, and thus seems a strong candidate for preventing late complications, TEVAR does not improve early survival. In addition, TEVAR is associated with a low but potentially devastating risk of procedural complications—such as stroke, paraplegia, and retrograde propagation of the dissection—which does not seem justified in many low-risk patients. Preemptive endografting of all patients with uncomplicated type-B AD may thus not be a better strategy than traditional OMT and surveillance. Risk stratification of these patients into those who might benefit from early TEVAR versus those who fare better with continued surveillance and OMT is thus highly desirable.

In this study, we demonstrate that a single clinical and 4 easily accessible morphological features identified by CT imaging at the time of the index hospitalization are strongly associated with late AEs. Based on these 5 variables, we have developed and internally validated a risk-prediction model which enables the calculation of the individual risk of AE, assuming that the baseline survival function is comparable with that in this study. Otherwise, patients can be ranked or classified into risk groups using the easily calculated linear predictor (risk score) with good discriminatory ability. This may be a first step toward a more nuanced and patient-centered alternative to the prevailing and currently evolving paradigms of exclusive OMT versus OMT+TEVAR in all patients with uncomplicated type-B AD.

The first and single clinical predictor of late AE in our patients was the presence of connective tissue disease such as the Marfan syndrome. This is an expected finding and presumably related to the inherently abnormal aortic tissue in these patients. The second risk factor—the first of the morphological predictors—was also an expected finding: Patients with an initially larger diameter of the dissected aorta are more likely to reach a critical thoracic aortic diameter which is associated with an increased risk of rupture and represents a consensual indication for treatment. The third significant risk factor, the circumferential extent of false lumen detachment, is a new parameter and was introduced as a more robust measure of the relative size of the false lumen within the dissected aorta. The circumferential extent of the false lumen reflects the proportion of the residual outer aortic wall characterized by reduced thickness and strength that is exposed to false lumen pressure. The extent of lesion could be a marker of more extensive preexisting aortic disease:

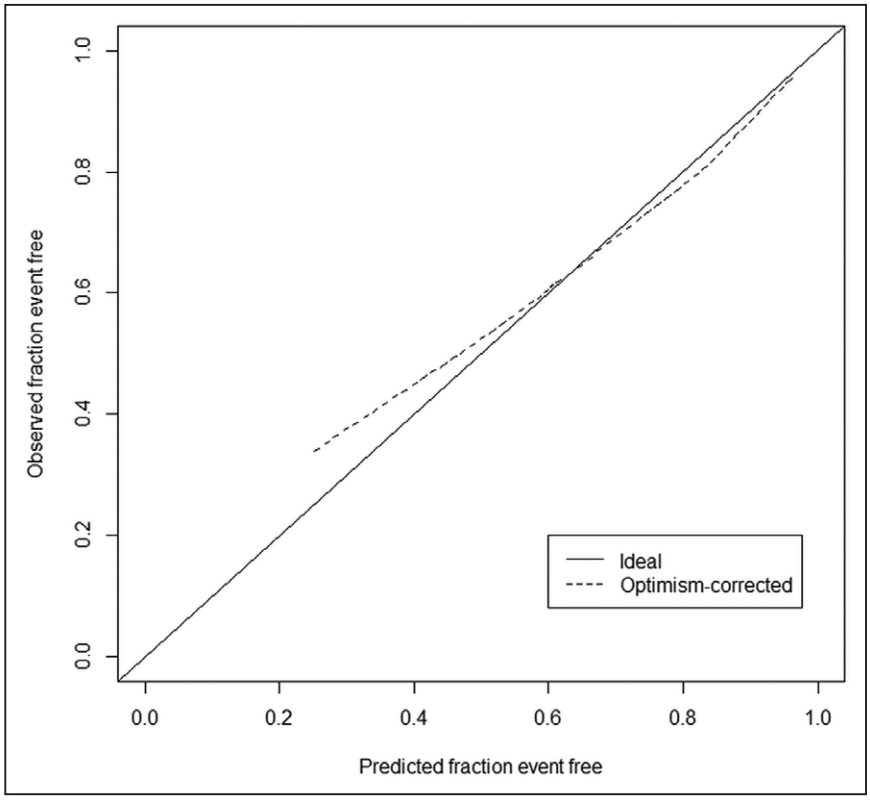

Figure 4. Calibration plot of the model obtained via resampling at 2 y follow-up. The number of bootstraps that were used was 1000. The optimism-corrected calibration line lies close to the line of perfect calibration. It shows a slight underestimation of risk for patients of relatively low risk of adverse events.

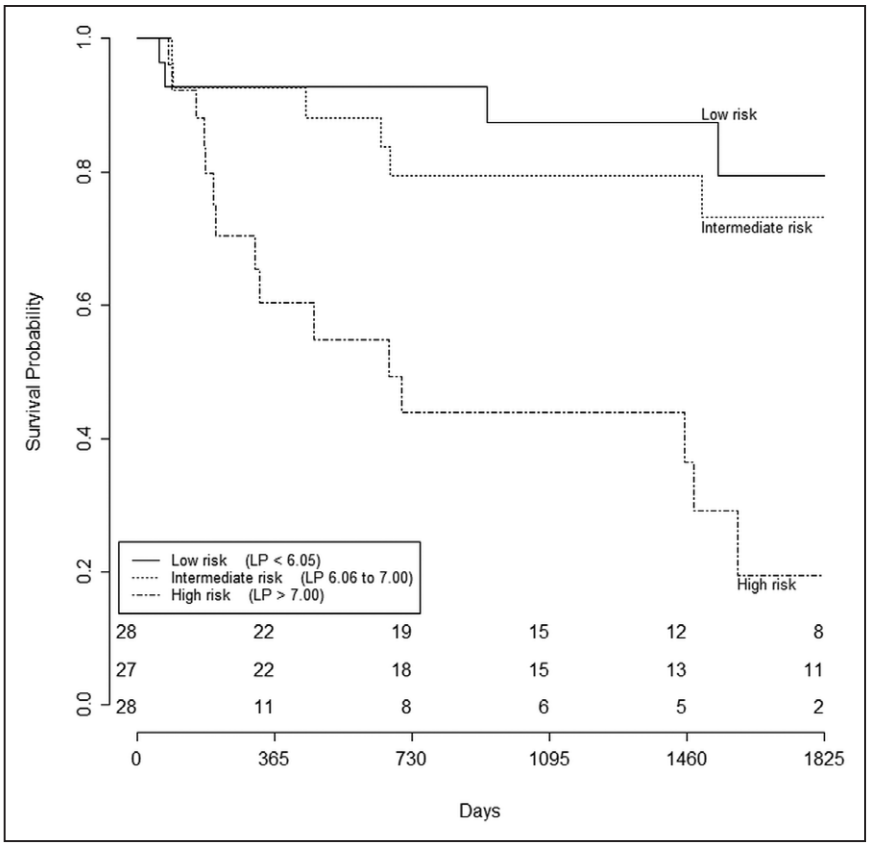

Figure 5. Kaplan–Meier curves of event-free survival stratified by tertile of the score on the linear predictor (LP). A score can be calculated using the internally validated model from Table 2 as: 0.841×(connective tissue disease)+0.021×(false lumen circumferential extent)+0.071×(maximum aortic diameter)−0.001×(false lumen outflow volume)−0.094×(number of intercostals). Note that the time-to-event data for each risk tertile are based on the same events used to create the model.

more cystic media disease would allow more extensive burrowing of blood into the diseased wall in the acute phase. The process might be amplified by the fact that increasing diameter is proportional to wall tension at same pressure, so a greater circumferential false lumen extent provides more tissue to dilate. The association with late complications is thus very plausible.

The final 2 significant morphological predictors are both new, both are protective, and both have been introduced with an intention to capture morphological features reflecting the hemodynamics of false lumen flow and pressurization. We found that greater drainage of the false lumen by large unobstructed branch arteries arising off the false lumen decreases the risk of AEs. This finding supports the hypothesis that insufficient outflow, or a mismatch between in- and outflow, may cause increased pressure in the false lumen, leading to either true lumen compression in the acute setting or false lumen expansion and aneurysm formation in the long run. This observation is also in keeping with experimental and clinical studies[30,41] demonstrating that pulsatile inflow into a lumen with impaired outflow may lead to a significant increase in the mean arterial and diastolic pressure as compared with a lumen with adequate outflow, despite similar systolic pressure.[34,36,42] Our findings are also consistent with the therapeutic strategy of intentionally increasing outflow from the false lumen either by septal fenestration or complete surgical or endovascular membrane removal to allow for luminal pressure equilibration. These concepts have been proposed 60 years ago by Shaw[43] and De Bakey et al[44] and are currently finding a revival.[41,45]

The last and somewhat unexpected morphological predictor—also protective—was the number of intercostal arteries arising from the dissected thoracic aorta. The intercostal arteries are the only outflow vessels at the level of the descending thoracic aorta—the region where false lumen aneurysms are most likely to occur. Although we were not able to reliably distinguish between intercostal arteries arising from the false versus the true lumen, the total number of intercostal arteries nonetheless proved to be a significant protective factor. One possible explanation of this unforeseen observation may be that with increasing number of intercostal arteries overall, the number of those arising from the false lumen presumably increases as well. With each intercostal artery originating from the false lumen, a small natural fenestration is also present, which may additionally create outflow from the false lumen, even if such a communication is too small to be identified with current CT technology in the acute phase. Because the number of intercostal arteries varied substantially among patients, another potential explanation may be that the number of patent intercostal arteries reflects better overall vascular status and a healthier vessel walls which could explain the protective nature of this parameter.

To illustrate how the magnitude of each of the above 5 predictor variables affects the absolute risk of an AE, we provide an online risk calculator under http://web.stanford.edu/group/3dq/cgi-bin/typeb-aortic-dissection-and-risk-calculator/calc-absolute/index.html. Although the risk calculator facilitates computation, it is currently based exclusively on our retrospective cohort and not externally validated. It is therefore not intended for clinical use.

The risk-prediction model shows good calibration and reasonable discriminative ability, with an optimism-corrected C statistic of 70.1%. Although the C statistic—as a global measure of discrimination over the entire follow-up period—indicates only a reasonable ability of the model to separate patients who will develop AEs from those who do not, the Kaplan–Meier risk analysis nicely demonstrates that the tertile of patients at highest risk of AEs is easiest to distinguish from the remaining groups. Identification of patients with high-risk scores would be clinically useful because high-risk patients might benefit most from a preemptive TEVAR strategy. To further illustrate the strength of our 5-parameter prediction model with its optimism-corrected C statistic of 70.1% in a clinical context, we also measured the model performance based on different predictors—those commonly associated with AEs in the literature: Connective tissue disease, aortic diameter >40 mm, false lumen diameter of ≥22 mm, and partial false lumen thrombosis, yielding individual C statistics of only 0.57, 0.57, 0.53, and 0.56, respectively. Even combining these 4 factors yielded an optimism-corrected C statistic of just 64.0%, markedly inferior to the prediction model presented in this article.

Limitations

This study has several limitations. The prediction model was developed in a retrospective cohort. Prospectively collected data with adequate long-term follow-up allowing the evaluation of late complications are currently not available. Our retrospective cohort from 2 large aortic centers allowed us to review high quality historic CT data obtained between 2002 and 2012 with long-term follow-up, from a time period when all cases of uncomplicated type-B ADs were initially treated conservatively. Approximately one-third of patients were lost to follow-up, mainly related to the fact that patients were transferred back to the referring facility for medical treatment and follow-up. The main considerations in the transition of care were related to the distance of patient residence or insurance coverage and therefore, a resultant selection bias related to the exclusion of this group of patients seems unlikely. Finally, the model has not yet been externally validated. The application of the model for clinical decision making in terms of patient selection for early preventive intervention can be considered after external validation with either retrospectively or prospectively collected data, for example, from the OMT arm of ongoing trials.

Although our findings suggest that hemodynamic information can be inferred from anatomic imaging features, it is important to keep in mind that the units of outflow in mL/min in our study are meant as a weighted score and should not be taken literally, because true flow measurements of blood flow have not been obtained. We also recognize that blood flow is more complex and varied among individuals. Reentry tears and natural fenestrations contribute to the complex individual flow and pressure dynamics which are not accounted for in the model, and small anatomic details may be completely undetected with current CT technology. Nevertheless, the observation that features related to false lumen outflow have predictive power suggest there is value in trying to better understand flow dynamics in ADs. Computational fluid dynamic modeling might be a tool to further explore such possibilities.

The presented risk model is based on morphological features observed exclusively in the acute phase. The risk scores therefore do not apply to imaging findings observed later during follow-up. Changes in feature morphology over time may very well have their own predictive power, however, and could be included into future models. Further research has to evaluate if such a model can further improve the prediction of AEs for non–high-risk patients based on additional information gained during follow-up imaging.

Conclusions

Morphological features on CT imaging in patients with acute uncomplicated type-B AD are strongly associated with late AE and can be used to predict individual risk of AE in an internally validated model. If externally validated this model may enable identification of high-risk patients who benefit most from early endovascular treatment, thus allowing a more individualized strategy than exclusive OMT or TEVAR in all patients in the future.

Acknowledgments

The authors thank Shannon G. Walters, MS, RT, from the Stanford 3D and Quantitative Imaging Laboratory for his support with the quantitative image analyses.

Sources of Funding

Dr Sailer is supported by the Koninklijke Nederlandse Akademie van Wetenschappen (Dutch Royal Society for Arts and Sciences); Dr Chiu is supported by a KL2 Mentored Career Development Award of the Stanford Clinical and Translational Science Award to Spectrum (NIH KL2 TR 001083). Dr Baeumler is supported by a Seed Grant from the Stanford Cardiovascular Institute, Stanford, CA. The project was supported by an National Institutes of Health Clinical and Translational Science Award UL1 RR025744.

Disclosures

None.

References

1. Hagan PG, Nienaber CA, Isselbacher EM, Bruckman D, Karavite DJ, Russman PL, Evangelista A, Fattori R, Suzuki T, Oh JK, Moore AG, Malouf JF, Pape LA, Gaca C, Sechtem U, Lenferink S, Deutsch HJ, Diedrichs H, Marcos y Robles J, Llovet A, Gilon D, Das SK, Armstrong WF, Deeb GM, Eagle KA. The International Registry of Acute Aortic Dissection (IRAD): new insights into an old disease. *JAMA*. 2000;283:897–903.
2. Estrera AL, Miller CC 3rd, Safi HJ, Goodrick JS, Keyhani A, Porat EE, Achouh PE, Meada R, Azizzadeh A, Dhareshwar J, Allaham A. Outcomes of medical management of acute type B aortic dissection. *Circulation*. 2006;114(1 suppl):I384–I389. doi: 10.1161/CIRCULATIONAHA.105.001479.
3. Tsai TT, Fattori R, Trimarchi S, Isselbacher E, Myrmel T, Evangelista A, Hutchison S, Sechtem U, Cooper JV, Smith DE, Pape L, Froehlich J, Raghupathy A, Januzzi JL, Eagle KA, Nienaber CA; International Registry of Acute Aortic Dissection. Long-term survival in patients presenting with type B acute aortic dissection: insights from the International Registry of Acute Aortic Dissection. *Circulation*. 2006;114:2226–2231. doi: 10.1161/CIRCULATIONAHA.106.622340.
4. Afifi RO, Sandhu HK, Leake SS, Boutrous ML, Kumar V 3rd, Azizzadeh A, Charlton-Ouw KM, Saqib NU, Nguyen TC, Miller CC 3rd, Safi HJ, Estrera AL. Outcomes of patients with acute type B (DeBakey III) aortic dissection: a 13-year, single-center experience. *Circulation*. 2015;132:748–754. doi: 10.1161/CIRCULATIONAHA.115.015302.

5. Pape LA, Awais M, Woznicki EM, Suzuki T, Trimarchi S, Evangelista A, Myrmel T, Larsen M, Harris KM, Greason K, Di Eusanio M, Bossone E, Montgomery DG, Eagle KA, Nienaber CA, Isselbacher EM, O'Gara P. Presentation, diagnosis, and outcomes of acute aortic dissection: 17-year trends from the International Registry of Acute Aortic Dissection. *J Am Coll Cardiol*. 2015;66:350–358. doi: 10.1016/j.jacc.2015.05.029.
6. Qin YL, Deng G, Li TX, Wang W, Teng GJ. Treatment of acute type-B aortic dissection: thoracic endovascular aortic repair or medical management alone? *JACC Cardiovasc Interv*. 2013;6:185–191. doi: 10.1016/j.jcin.2012.11.004.
7. DeBakey ME, McCollum CH, Crawford ES, Morris GC Jr, Howell J, Noon GP, Lawrie G. Dissection and dissecting aneurysms of the aorta: twenty-year follow-up of five hundred twenty-seven patients treated surgically. *Surgery*. 1982;92:1118–1134.
8. Juvonen T, Ergin MA, Galla JD, Lansman SL, McCullough JN, Nguyen K, Bodian CA, Ehrlich MP, Spielvogel D, Klein JJ, Griepp RB. Risk factors for rupture of chronic type B dissections. *J Thorac Cardiovasc Surg*. 1999;117:776–786. doi: 10.1016/S0022-5223(99)70299-0.
9. Durham CA, Cambria RP, Wang LJ, Ergul EA, Aranson NJ, Patel VI, Conrad MF. The natural history of medically managed acute type B aortic dissection. *J Vasc Surg*. 2015;61:1192–1198. doi: 10.1016/j.jvs.2014.12.038.
10. Akin I, Kische S, Rehders TC, Ince H, Nienaber CA. Thoracic endovascular stent-graft therapy in aortic dissection. *Curr Opin Cardiol*. 2010;25:552–559. doi: 10.1097/HCO.0b013e32833e6dd8.
11. Patterson BO, Cobb RJ, Karthikesalingam A, Holt PJ, Hinchliffe RJ, Loftus IM, Thompson MM. A systematic review of aortic remodeling after endovascular repair of type B aortic dissection: methods and outcomes. *Ann Thorac Surg*. 2014;97:588–595. doi: 10.1016/j.athoracsur.2013.07.128.
12. Fanelli F, Cannavale A, O'Sullivan GJ, Gazzetti M, Cirelli C, Lucatelli P, Santoni M, Catalano C. Endovascular repair of acute and chronic aortic type B dissections: main factors affecting aortic remodeling and clinical outcome. *JCC. Cardiovasc Interv*. 2016;9:183–191. doi: 10.1016/j.jcin.2015.10.027.
13. Brunkwall J, Kasprzak P, Verhoeven E, Heijmen R, Taylor P; ADSORB Trialists. Endovascular repair of acute uncomplicated aortic type B dissection promotes aortic remodelling: 1 year results of the ADSORB trial. *Eur J Vasc Endovasc Surg*. 2014; 48:285–91.
14. Nienaber CA, Rousseau H, Eggebrecht H, Kische S, Fattori R, Rehders TC, Kundt G, Scheinert D, Czerny M, Kleinfeldt T, Zipfel B, Labrousse L, Ince H; INSTEAD Trial. Randomized comparison of strategies for type B aortic dissection: the INvestigation of STEnt Grafts in Aortic Dissection (INSTEAD) trial. *Circulation*. 2009;120:2519–2528. doi: 10.1161/CIRCULATIONAHA.109.886408.
15. Walsh SR, Tang TY, Sadat U, Naik J, Gaunt ME, Boyle JR, Hayes PD, Varty K. Endovascular stenting versus open surgery for thoracic aortic disease: systematic review and meta-analysis of perioperative results. *J Vasc Surg*. 2008;47:1094–1098. doi: 10.1016/j.jvs.2007.09.062.
16. Cooper DG, Walsh SR, Sadat U, Noorani A, Hayes PD, Boyle JR. Neurological complications after left subclavian artery coverage during thoracic endovascular aortic repair: a systematic review and meta-analysis. *J Vasc Surg*. 2009;49:1594–1601. doi: 10.1016/j.jvs.2008.12.075.
17. Wong CS, Healy D, Canning C, Coffey JC, Boyle JR, Walsh SR. A systematic review of spinal cord injury and cerebrospinal fluid drainage after thoracic aortic endografting. *J Vasc Surg*. 2012;56:1438–1447. doi: 10.1016/j.jvs.2012.05.075.
18. Bernard Y, Zimmermann H, Chocron S, Litzler JF, Kastler B, Etievent JP, Meneveau N, Schiele F, Bassand JP. False lumen patency as a predictor of late outcome in aortic dissection. *Am J Cardiol*. 2001;87:1378–1382.
19. Trimarchi S, Tolenaar JL, Jonker FH, Murray B, Tsai TT, Eagle KA, Rampoldi V, Verhagen HJ, van Herwaarden JA, Moll FL, Muhs BE, Elefteriades JA. Importance of false lumen thrombosis in type B aortic dissection prognosis. *J Thorac Cardiovasc Surg*. 2013;145(3 suppl):S208–S212. doi: 10.1016/j.jtcvs.2012.11.048.
20. Tanaka A, Sakakibara M, Ishii H, Hayashida R, Jinno Y, Okumura S, Okada K, Murohara T. Influence of the false lumen status on clinical outcomes in patients with acute type B aortic dissection. *J Vasc Surg*. 2014;59:321–326. doi: 10.1016/j.jvs.2013.08.031.
21. Grommes J, Greiner A, Bendermacher B, Erlmeier M, Frech A, Belau P, Kennes LN, Fraedrich G, Schurink GW, Jacobs MJ, Klocker J. Risk factors for mortality and failure of conservative treatment after aortic type B dissection. *J Thorac Cardiovasc Surg*. 2014; 148:2155–2160.e1.
22. Sueyoshi E, Sakamoto I, Hayashi K, Yamaguchi T, Imada T. Growth rate of aortic diameter in patients with type B aortic dissection during the chronic phase. *Circulation*. 2004;110(11 suppl 1):II256–II261. doi: 10.1161/01.CIR.0000138386.48852.b6.
23. Takahashi J, Wakamatsu Y, Okude J, Kanaoka T, Sanefuji Y, Gohda T, Sasaki S, Matsui Y. Maximum aortic diameter as a simple predictor of acute type B aortic dissection. *Ann Thorac Cardiovasc Surg*. 2008;14:303–310.
24. Tsai TT, Evangelista A, Nienaber CA, Myrmel T, Meinhardt G, Cooper JV, Smith DE, Suzuki T, Fattori R, Llovet A, Froehlich J, Hutchison S, Distante A, Sundt T, Beckman J, Januzzi JL Jr, Isselbacher EM, Eagle KA; International Registry of Acute Aortic Dissection. Partial thrombosis of the false lumen in patients with acute type B aortic dissection. *N Engl J Med*. 2007;357:349–359. doi: 10.1056/NEJMoa063232.
25. Evangelista A, Salas A, Ribera A, Ferreira-González I, Cuellar H, Pineda V, González-Alujas T, Bijnens B, Permanyer-Miralda G, Garcia-Dorado D. Long-term outcome of aortic dissection with patent false lumen: predictive role of entry tear size and location. *Circulation*. 2012;125:3133–3141. doi: 10.1161/CIRCULATIONAHA.111.090266.
26. Tolenaar JL, van Keulen JW, Trimarchi S, Jonker FH, van Herwaarden JA, Verhagen HJ, Moll FL, Muhs BE. Number of entry tears is associated with aortic growth in type B dissections. *Ann Thorac Surg*. 2013;96:39–42. doi: 10.1016/j.athoracsur.2013.03.087.
27. Song JM, Kim SD, Kim JH, Kim MJ, Kang DH, Seo JB, Lim TH, Lee JW, Song MG, Song JK. Long-term predictors of descending aorta aneurysmal change in patients with aortic dissection. *J Am Coll Cardiol*. 2007;50:799–804. doi: 10.1016/j.jacc.2007.03.064.
28. Weiss G, Wolner I, Folkmann S, Sodeck G, Schmidli J, Grabenwöger M, Carrel T, Czerny M. The location of the primary entry tear in acute type B aortic dissection affects early outcome. *Eur J Cardiothorac Surg*. 2012;42:571–576. doi: 10.1093/ejcts/ezs056.
29. Marui A, Mochizuki T, Koyama T, Mitsui N. Degree of fusiform dilatation of the proximal descending aorta in type B acute aortic dissection can predict late aortic events. *J Thorac Cardiovasc Surg*. 2007;134:1163–1170. doi: 10.1016/j.jtcvs.2007.07.037.
30. Winnerkvist A, Lockowandt U, Rasmussen E, Rådegran K. A prospective study of medically treated acute type B aortic dissection. *Eur J Vasc Endovasc Surg*. 2006;32:349–355. doi: 10.1016/j.ejvs.2006.04.004.
31. Tolenaar JL, van Keulen JW, Jonker FH, van Herwaarden JA, Verhagen HJ, Moll FL, Muhs BE, Trimarchi S. Morphologic predictors of aortic dilatation in type B aortic dissection. *J Vasc Surg*. 2013;58:1220–1225. doi: 10.1016/j.jvs.2013.05.031.
32. van Bogerijen GH, Tolenaar JL, Rampoldi V, Moll FL, van Herwaarden JA, Jonker FH, Eagle KA, Trimarchi S. Predictors of aortic growth in uncomplicated type B aortic dissection. *J Vasc Surg*. 2014;59:1134–1143. doi: 10.1016/j.jvs.2014.01.042.
33. Chau KH, Elefteriades JA. Natural history of thoracic aortic aneurysms: size matters, plus moving beyond size. *Prog Cardiovasc Dis*. 2013;56:74–80. doi: 10.1016/j.pcad.2013.05.007.
34. Chung JW, Elkins C, Sakai T, Kato N, Vestring T, Semba CP, Slonim SM, Dake MD. True-lumen collapse in aortic dissection: part I. Evaluation of causative factors in phantoms with pulsatile flow. *Radiology*. 2000;214:87–98. doi: 10.1148/radiology.214.1.r00ja3287.
35. Chung JW, Elkins C, Sakai T, Kato N, Vestring T, Semba CP, Slonim SM, Dake MD. True-lumen collapse in aortic dissection: part II. Evaluation of treatment methods in phantoms with pulsatile flow. *Radiology*. 2000;214:99–106. doi: 10.1148/radiology.214.1.r00ja3499.
36. Williams DM, Lee DY, Hamilton BH, Marx MV, Narasimham DL, Kazanjian SN, Prince MR, Andrews JC, Cho KJ, Deeb GM. The dissected aorta: part III. Anatomy and radiologic diagnosis of branch-vessel compromise. *Radiology*. 1997;203:37–44. doi: 10.1148/radiology.203.1.9122414.
37. Williams LR, Leggett RW. Reference values for resting blood flow to organs of man. *Clin Phys Physiol Meas*. 1989;10:187–217.
38. Steyerberg EW. *Clinical prediction models: a practical approach to development, validation, and updating*. New York, NY: Springer; 2009.
39. Harrell FE. *Regression modeling strategies: with applications to linear models, logistic regression, and survival analysis*. New York: Springer; 2001.
40. Steyerberg EW, Harrell FE Jr, Borsboom GJ, Eijkemans MJ, Vergouwe Y, Habbema JD. Internal validation of predictive models: efficiency of some procedures for logistic regression analysis. *J Clin Epidemiol*. 2001;54:774–781.
41. Berguer R, Parodi JC, Schlicht M, Khanafer K. Experimental and clinical evidence supporting septectomy in the primary treatment of acute type B thoracic aortic dissection. *Ann Vasc Surg*. 2015;29:167–173. doi: 10.1016/j.avsg.2014.10.001.

42. Parodi JC, Berguer R, Ferreira LM, La Mura R, Schermerhorn ML. Intra-aneurysmal pressure after incomplete endovascular exclusion. *J Vasc Surg*. 2001;34:909–914. doi: 10.1067/mva.2001.119038.
43. Shaw RS. Acute dissecting aortic aneurysm; treatment by fenestration of the internal wall of the aneurysm. *N Engl J Med*. 1955;253:331–333. doi: 10.1056/NEJM195508252530807.
44. De Bakey ME, Cooley DA, Creech O Jr. Surgical considerations of dissecting aneurysm of the aorta. *Ann Surg*. 1955; 142:586–610; discussion, 611–612.
45. Veger HT, Westenberg JJ, Visser MJ. The role of branch vessels in aortic type B dissection: an *in vitro* study. *Eur J Vasc Endovasc Surg*. 2015;49:375–381. doi: 10.1016/j.ejvs.2014.12.016.

CLINICAL PERSPECTIVE

Traditional medical treatment of patients with uncomplicated type-B aortic dissection is associated with a high rate of late adverse events, which might be prevented by thoracic endovascular aortic repair. In this retrospective work, we examined clinical and multiple imaging features extracted from computed tomogrpahy scans obtained during the index hospitalization to develop a prediction model for late adverse events, such as aortic rupture, rapid aortic growth, aneurysm formation, new organ or limb ischemia, or new uncontrollable hypertension or pain. We found 5 predictors—4 from imaging—associated with late adverse events with a median follow-up of 850 days: connective tissue disease, maximum aortic diameter, circumferential extent of the aortic false lumen, false lumen outflow, and number of intercostal arteries. The model was internally validated by bootstrapping and showed good discriminatory ability with an optimism-corrected C statistic of 70.1%. If externally validated, these findings may allow identifying patients at increased risk for late adverse events and thus help to determine which patients might benefit from preventive endografting in the future.

Circulation
Cardiovascular Imaging

Computed Tomography Imaging Features in Acute Uncomplicated Stanford Type-B Aortic Dissection Predict Late Adverse Events

Anna M. Sailer, Sander M.J. van Kuijk, Patricia J. Nelemans, Anne S. Chin, Aya Kino, Mark Huininga, Johanna Schmidt, Gabriel Mistelbauer, Kathrin Bäumler, Peter Chiu, Michael P. Fischbein, Michael D. Dake, D. Craig Miller, Geert Willem H. Schurink and Dominik Fleischmann

Circ Cardiovasc Imaging. 2017;10:
doi: 10.1161/CIRCIMAGING.116.005709
Circulation: Cardiovascular Imaging is published by the American Heart Association, 7272 Greenville Avenue, Dallas, TX 75231

Print ISSN: 1941-9651. Online ISSN: 1942-0080